

# Tuning the silver(I) complexes of 3-(2-pyridyl)pyrazole-based ligands: Syntheses and crystal structures of the complexes, as well as theoretical investigations on the coordination abilities of the ligands

Chun-Sen Liu, Jian-Rong Li, Ru-Qiang Zou, Jiang-Ning Zhou, Xue-Song Shi,  
Jun-Jie Wang, Xian-He Bu \*

*Department of Chemistry, Nankai University, Tianjin 300071, People's Republic of China*

Received 14 October 2006; received in revised form 17 December 2006; accepted 19 December 2006

Available online 10 January 2007

## Abstract

In our efforts to investigate the influences of different pendant aromatic groups and the spatial position of N donors in 3-(2-pyridyl)pyrazole-based ligands on the structures of their metal complexes, five structurally related ligands: 1-[3-(2-pyridyl)pyrazol-1-ylmethyl]benzene ( $L^1$ ), 1-[3-(2-pyridyl)pyrazol-1-ylmethyl]naphthalene ( $L^2$ ), 8-[3-(2-pyridyl)pyrazol-1-ylmethyl]quinoline ( $L^3$ ), 3-[3-(2-pyridyl)pyrazol-1-ylmethyl]pyridine ( $L^4$ ) and 4-[3-(2-pyridyl)pyrazol-1-ylmethyl]pyridine ( $L^5$ ), have been used to react with  $AgClO_4$  to form five Ag(I) complexes,  $[Ag(L^1)_2](ClO_4)$  (**1**),  $[Ag(L^2)_2](ClO_4)$  (**2**),  $[Ag(L^3)(HL^3)](ClO_4)_2(CH_3CN)$  (**3**),  $\{[Ag(L^4)](ClO_4)\}_2$  (**4**), and  $\{[Ag(L^5)](ClO_4)\}_\infty$  (**5**). The structural differences of these complexes may be attributed to the coordination geometries or N donor position of the pendant aromatic groups in ligands  $L^1$ – $L^5$ . Also, the result reveals that various intra- and/or inter-molecular weak interactions, such as  $\pi \cdots \pi$  stacking, C–H $\cdots\pi$  and C–H $\cdots$ O H-bonding interactions, play important roles in the formation of **1**–**5**, especially in the aspect of linking the multi-nuclear discrete subunits or low-dimensional entities into high-dimensional frameworks. Moreover, the coordination behaviors of ligands  $L^1$ – $L^5$  have been briefly evaluated by DFT calculations.

© 2007 Elsevier B.V. All rights reserved.

**Keywords:** 3-(2-Pyridyl)pyrazole-based ligands; Ag(I) complexes; Crystal structures; DFT calculations

## 1. Introduction

The synthesis of multi-nuclear discrete or infinite coordination architectures has attracted great interest in coordination and supramolecular chemistry due to their intriguing structures and potential applications as functional materials [1–3]. The formation of these coordination architectures depends mainly on the combinations of two factors including the coordination geometry of metal ions and the nature of ligands [4]. However, the methodologies to use transition metal ions as connecting nodes to hold together organic ligands in predefined patterns within self-assembled oligomeric or polymeric aggregates still remains a great challenge

[5,6]. Indeed, in addition to coordination bonding [7,8], some weak intra- or inter-molecular interactions, such as H-bonding [9–13] and  $\pi \cdots \pi$  stacking [14–16] also affect the final structures of coordination complexes, and they may further link discrete subunits or low-dimensional entities into high-dimensional supramolecular networks [3–6].

Ward et al. has initially reported many coordination architectures of 3-(2-pyridyl)pyrazole and its derivative ligands [17]. In our recent work, a series of 3-(2-pyridyl)pyrazole-based ligands have been also used to construct complexes with various structures including multi-nuclear discrete molecules as well as one-dimensional (1D) and two-dimensional (2D) coordination polymers exhibiting interesting properties [18]. In order to further investigate the coordination architectures of such ligands, five structurally related 3-(2-pyridyl)pyrazole-based ligands,

\* Corresponding author. Tel.: +86 22 23502809; fax: +86 22 23502458.  
E-mail address: [buxh@nankai.edu.cn](mailto:buxh@nankai.edu.cn) (X.-H. Bu).

1-[3-(2-pyridyl)pyrazol-1-ylmethyl]benzene (**L**<sup>1</sup>), 1-[3-(2-pyridyl)pyrazol-1-ylmethyl]naphthalene (**L**<sup>2</sup>), 8-[3-(2-pyridyl)pyrazol-1-ylmethyl]quinoline (**L**<sup>3</sup>), 3-[3-(2-pyridyl)pyrazol-1-ylmethyl]pyridine (**L**<sup>4</sup>) and 4-[3-(2-pyridyl)pyrazol-1-ylmethyl]pyridine (**L**<sup>5</sup>), have been synthesized (Chart 1), and their reactions with AgClO<sub>4</sub>·H<sub>2</sub>O offered five complexes, [Ag(**L**<sup>1</sup>)<sub>2</sub>](ClO<sub>4</sub>) (**1**), [Ag(**L**<sup>2</sup>)<sub>2</sub>](ClO<sub>4</sub>) (**2**), [Ag(**L**<sup>3</sup>)(HL<sup>3</sup>)](ClO<sub>4</sub>)<sub>2</sub>(CH<sub>3</sub>CN) (**3**), {[Ag(**L**<sup>4</sup>)](ClO<sub>4</sub>)<sub>2</sub>} (**4**) and {[Ag(**L**<sup>5</sup>)](ClO<sub>4</sub>)<sub>2</sub>}<sub>∞</sub> (**5**). These complexes have different structures, showing the influences of the coordination geometries of the pendant groups in **L**<sup>1</sup>–**L**<sup>5</sup> ligands. Furthermore, DFT theoretical calculations have also been carried out for briefly estimating the coordination abilities of such ligands.

## 2. Experimental

### 2.1. Materials and general methods

3-(2-Pyridyl)pyrazole [19a,19b,19c] and 8-bromomethylquinoline [19d] were synthesized according to the reported

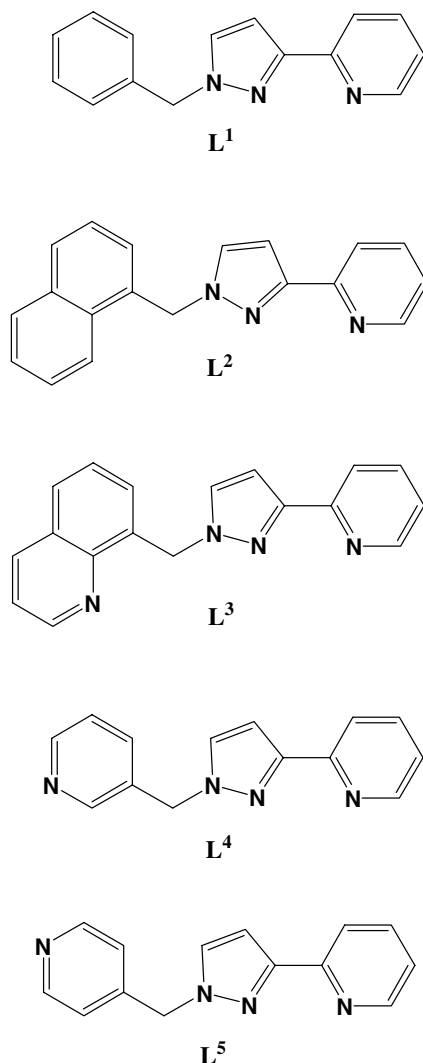


Chart 1.

procedures. All the other reagents for synthesis were commercially available and used as received or purified by standard methods prior to use. Melting points were measured on an X-4 micro melting point detector without further correction. Elemental analyses (C, H, and N) were performed on a Perkin-Elmer 240C analyzer and IR spectra were measured on a Tensor 27 OPUS (Bruker) FT-IR spectrometer with KBr pellets. <sup>1</sup>H NMR spectra were recorded on a Bruker AC-P500 spectrometer (300 MHz) at 25 °C in CDCl<sub>3</sub> with tetramethylsilane as the internal reference.

### 2.2. Syntheses of ligands

The ligands **L**<sup>1</sup>–**L**<sup>5</sup> were prepared by modified literature procedures [18,20]. The reactions of 3-(2-pyridyl)pyrazole with benzyl chloride, 1-(chloromethyl)naphthalene, 8-bromomethylquinoline, 3-(chloromethyl)pyridine hydrochloride (3-picoyl chloride hydrochloride) and 4-(chloromethyl)pyridine hydrochloride (4-picoyl chloride hydrochloride), respectively, in benzene as well as in the presence of NaOH and <sup>n</sup>Bu<sub>4</sub>NOH, gave ligands **L**<sup>1</sup>–**L**<sup>5</sup>. It should be pointed out that **L**<sup>1</sup> along with its related metal complexes has been synthesized and reported by us [18a] and others [20c], meanwhile, **L**<sup>2</sup> and its Cu(II), Zn(II) and Cd(II) complexes [18b,18c] as well as **L**<sup>3</sup> and its Cu(II) complex [18d] have also been documented in our previous work. Also, the structure of the copper acetate complex [18d] of **L**<sup>3</sup> is similar to the Ag(I) complex **3** described in this work.

For **L**<sup>4</sup>, yield: ~30%. Mp.: 78–80 °C. <sup>1</sup>H NMR (300 MHz, CDCl<sub>3</sub>): δ 5.54 (s, 2H), 6.95 (d, *J* = 2.4 Hz, 1H), 7.05 (d, *J* = 6.9 Hz, 1H), 7.18–7.23 (m, 2H), 7.59 (d, *J* = 2.4 Hz, 1H), 7.60–7.74 (m, 2H), 7.95 (d, *J* = 7.8 Hz, 1H), 8.58–8.64 (m, 2H). IR (cm<sup>-1</sup>): 3111w, 1594s, 1494m, 1458m, 1432s, 1355m, 1271m, 1247m, 1057m, 1030m, 994m, 789vs, 756s, 704m. Anal. Calcd for C<sub>14</sub>H<sub>12</sub>N<sub>4</sub>: C, 71.17; H, 5.12; N, 23.71. Found: C, 71.23; H, 4.98; N, 23.92%.

For **L**<sup>5</sup>, yield: ~30%. Mp: 81–83 °C. <sup>1</sup>H NMR (300 MHz, CDCl<sub>3</sub>): δ 5.43 (s, 2H), 7.01 (d, *J* = 2.4 Hz, 1H), 7.08 (d, *J* = 6.3 Hz, 2H), 7.21–7.25 (m, 1H), 7.51 (d, *J* = 2.4 Hz, 1H), 7.71–7.77 (m, 1H), 7.95 (d, *J* = 7.8 Hz, 1H), 8.56–8.59 (m, 2H), 8.64–8.66 (m, 1H). IR (KBr, cm<sup>-1</sup>): 2890w, 2790w, 1592s, 1566m, 1487s, 1458s, 1399m, 1277m, 1220vs, 1049s, 991m, 800m, 759s, 620m. Anal. Calcd for C<sub>14</sub>H<sub>12</sub>N<sub>4</sub>: C, 71.17; H, 5.12; N, 23.71. Found: C, 70.95; H, 5.24; N, 23.91%.

### 2.3. Synthesis of complexes 1–5

All measurements were performed based on the crystal samples.

[Ag(**L**<sup>1</sup>)<sub>2</sub>](ClO<sub>4</sub>) (**1**). The reaction of **L**<sup>1</sup> (0.1 mmol) with AgClO<sub>4</sub>·H<sub>2</sub>O (0.1 mmol) in MeOH (10 ml) for a few minutes afforded the yellow solid, which was then filtered. The resulted solution was kept at room temperature in the dark. Yellow single crystals were obtained by slow evaporation of the solvent after several days. Yield: ~40%. IR

Table 1  
Crystallographic data and structure refinement summary for complexes 1–5

	1	2	3	4	5
Chemical formula	C <sub>30</sub> H <sub>26</sub> AgClN <sub>6</sub> O <sub>4</sub>	C <sub>38</sub> H <sub>30</sub> AgClN <sub>6</sub> O <sub>4</sub>	C <sub>38</sub> H <sub>32</sub> AgCl <sub>2</sub> N <sub>9</sub> O <sub>8</sub>	C <sub>28</sub> H <sub>24</sub> Ag <sub>2</sub> Cl <sub>2</sub> N <sub>8</sub> O <sub>8</sub>	C <sub>14</sub> H <sub>12</sub> AgClN <sub>4</sub> O <sub>4</sub>
Formula weight	677.89	778.00	921.50	887.20	443.60
Crystal system	Monoclinic	Orthorhombic	Monoclinic	Triclinic	Monoclinic
Space group	<i>P</i> 2(1)/ <i>c</i>	<i>Pna</i> 2(1)	<i>P</i> 2(1)/ <i>c</i>	<i>P</i> –1	<i>P</i> 2(1)/ <i>c</i>
<i>a</i> (Å)	10.892(3)	14.585(5)	15.946(3)	7.700(3)	13.162(2)
<i>b</i> (Å)	11.940(3)	16.620(5)	17.292(3)	9.264(3)	8.1298(1)
<i>c</i> (Å)	22.380(7)	13.782(4)	14.140(3)	11.609(4)	14.888(2)
$\alpha$ (°)	90	90	90	91.763(5)	90
$\beta$ (°)	92.642(5)	90	107.101(3)	99.740(5)	90.348(3)
$\gamma$ (°)	90	90	90	102.660(5)	90
<i>V</i> (Å <sup>3</sup> )	2907.3(15)	3340.7(19)	3726.6(12)	794.3(5)	1593.1(4)
<i>Z</i>	4	4	4	1	4
<i>D</i> (g cm <sup>–3</sup> )	1.549	1.547	1.642	1.855	1.850
$\mu$ (mm <sup>–1</sup> )	0.832	0.735	0.752	1.464	1.460
GOF	1.004	0.946	0.723	1.040	1.013
<i>T</i> (K)	293(2)	293(2)	293(2)	293(2)	293(2)
<i>R</i> <sup>a</sup> / <i>wR</i> <sup>b</sup> [ <i>I</i> > 2 $\sigma$ ( <i>I</i> )]	0.0570/0.1318	0.0456/0.0582	0.0422/0.0563	0.0308/0.0705	0.0322/0.0654

$$^a R = \frac{\sum(|F_0| - |F_C|)}{\sum|F_0|}$$

$$^b wR = \left[ \frac{\sum w(|F_0|^2 - |F_C|^2)^2}{\sum w(F_0^2)} \right]^{1/2}$$

(cm<sup>–1</sup>): 3134*w*, 1600*s*, 1569*w*, 1498*s*, 1456*w*, 1434*s*, 1372*w*, 1358*w*, 1333*w*, 1236*s*, 1101*vs*, 959*w*, 774*s*, 722*s*, 705*w*, 621*m*, 460*w*. Anal. Calcd for C<sub>30</sub>H<sub>26</sub>AgClN<sub>6</sub>O<sub>4</sub>: C, 53.15; H, 3.87; N, 12.40. Found: C, 52.87; H, 4.06; N, 12.01.

[Ag(L<sup>2</sup>)<sub>2</sub>](ClO<sub>4</sub>) (**2**). Yellow single crystals of **2** were obtained by the similar method as described for **1** except for L<sup>2</sup> replacing L<sup>1</sup>. Yield: ~50%. IR (cm<sup>–1</sup>): 3110*w*, 3041*w*, 1592*s*, 1563*br*, 1512*w*, 1459*s*, 1401*m*, 1385*m*,

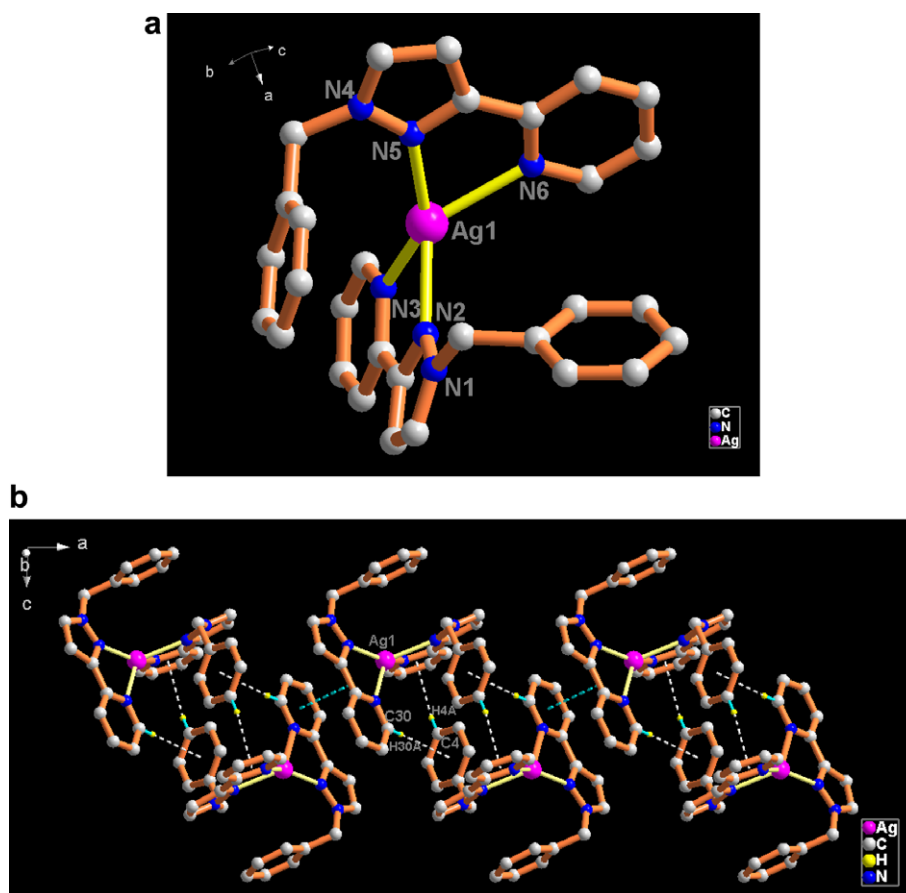


Fig. 1. View of (a) the coordination environment of Ag(I) in **1** and (b) the 1D chain formed by the intermolecular C–H... $\pi$  and  $\pi$ ... $\pi$  interactions (partial H atoms and ClO<sub>4</sub><sup>–</sup> omitted for clarity).

1357m, 1326m, 1276w, 1233s, 1151m, 1113w, 1092m, 1053s, 993m, 959w, 860w, 793s, 776vs, 743s, 723m, 621m, 533w, 420w. Anal. Calcd for  $C_{38}H_{30}AgClN_6O_4$ : C, 58.66; H, 3.89; N, 10.80. Found: C, 58.34; H, 3.91; N, 11.05.

$[Ag(L^3)(HL^3)](ClO_4)_2(CH_3CN)$  (**3**). Mixing  $L^3$  (0.1 mmol) and  $AgClO_4 \cdot H_2O$  (0.1 mmol) in a mixed solution of MeOH and  $H_2O$  (v/v = 1:1) to obtain yellow solid which was filtered and washed with acetone and dried in air. Single crystals were obtained by slow diffusion of  $Et_2O$  into the acetonitrile solution of the solid. Yield: ~40%. IR ( $cm^{-1}$ ): 3105w, 3022w, 2841w, 1690vs, 1506s, 1468vs, 1143vs, 1097s, 864s, 780s, 623s. Anal. Calcd for  $C_{38}H_{32}AgCl_2N_9O_8$ : C, 49.53; H, 3.50; N, 13.68. Found: C, 49.21; H, 3.41; N, 14.05.

$\{[Ag(L^4)](ClO_4)\}_2$  (**4**). Similar synthetic procedure as for **3** was used except that  $L^3$  was replaced by  $L^4$ , giving yellow single crystals. Yield: ~40%. IR ( $cm^{-1}$ ): 3147w, 1602s, 1523w, 1504w, 1434s, 1361m, 1321w, 1242s, 1197m, 1080vs, 767s, 708w, 622s. Anal. Calcd for  $C_{28}H_{24}Ag_2Cl_2N_8O_8$ : C, 37.91; H, 2.73; N, 12.63. Found: C, 38.01; H, 2.83; N, 12.24%.

$\{[Ag(L^5)](ClO_4)\}_\infty$  (**5**). Similar synthetic procedure as for **3** was also used except that  $L^3$  was replaced by  $L^5$ , and **5** was obtained as yellow single crystals. Yield: ~30%. IR ( $cm^{-1}$ ): 3167w, 1595m, 1499w, 1429s, 1360m, 1324m, 1240m, 1078vs, 780s, 718w, 621s, 474w. Anal. Calcd for  $C_{14}H_{12}AgClN_4O_4$ : C, 37.91; H, 2.73; N, 12.63. Found: C, 37.50; H, 2.71; N, 12.32%.

**Caution!** Although we have met no problems in handling perchlorate salt during this work, these should be treaded cautiously owing to their potential explosive nature.

#### 2.4. X-ray crystallographic studies of 1–5

X-ray single-crystal diffraction data for complexes **1–5** were collected on a Bruker Smart 1000 CCD diffractometer at 293(2) K with Mo-K $\alpha$  radiation ( $\lambda = 0.71073$  Å). The program SAINT [21] was used for integration of the diffraction profiles. Semi-empirical absorption corrections were applied using SADABS program [22]. All the structures were solved by direct methods using the SHELXS program of the SHELXTL [23] package and refined by full-matrix least-squares methods with SHELXL. Metal atoms in each complex were located from the *E*-maps, and other non-hydrogen atoms were located in successive difference Fourier syntheses and refined with anisotropic thermal parameters on  $F^2$ . The hydrogen atoms of the ligands were generated theoretically onto the specific atoms and refined isotropically with fixed thermal factors. Crystallographic data and experimental details for structural analyses are summarized in Table 1. These crystallographic data files in CIF format were deposited in Cambridge Crystallographic Data Center (CCDC Nos. 606061–606065 for **1–5**). These data can be obtained from the Cambridge Crystallographic Data Centre, 12 Union Road, Cambridge CB2 1EZ, UK; Fax: +44 1223 336033; e-mail: deposit@ccdc.cam.ac.uk.

#### 2.5. Calculation details

The molecular mechanics optimization of the ligands  $L^1$ – $L^5$  was carried out by DFT based on the structures obtained from the crystallographic data and the termination condition is that the RMS gradient is below 0.01 kcal/mol. Then the Gaussian 03 set of programs was applied to perform quantum-chemical computation of the  $MM^+$ -optimized ligands [24]. The  $MM^+$ -optimized ligands were further fully optimized using density functional theory (DFT) method with B3LYP exchange-correlation functional [25] and 6-31G (d, p) basis set, respectively. Also, to ensure that the stationary points located on the potential energy surfaces were minima, the vibrational frequency calculations were done.

### 3. Results and discussion

#### 3.1. Synthesis and general characterizations

Complexes **1–5** were prepared by the reaction of  $AgClO_4 \cdot H_2O$  and ligands  $L^1$ – $L^5$  under similar conditions. The IR spectra for the five complexes show absorption bands resulting from the skeletal vibrations of the aromatic rings in 1600–1400  $cm^{-1}$  region, and the characteristic bands of perchlorate anions at ~620 and ~1100  $cm^{-1}$ . It should be noted that, due to the coordination of the

Table 2  
Selected bond distances (Å) and angles (°) for complexes **1–5**

<i>Complex 1</i>			
Ag(1)–N(5)	2.253(4)	Ag(1)–N(3)	2.275(4)
Ag(1)–N(2)	2.360(4)	Ag(1)–N(6)	2.416(4)
N(5)–Ag(1)–N(3)	146.05(16)	N(5)–Ag(1)–N(2)	123.83(14)
N(3)–Ag(1)–N(2)	72.31(15)	N(5)–Ag(1)–N(6)	71.20(15)
N(3)–Ag(1)–N(6)	132.47(15)	N(2)–Ag(1)–N(6)	116.32(13)
<i>Complex 2</i>			
Ag(1)–N(5)	2.293(5)	Ag(1)–N(2)	2.302(3)
Ag(1)–N(6)	2.370(5)	Ag(1)–N(3)	2.371(3)
N(5)–Ag(1)–N(2)	138.46(17)	N(5)–Ag(1)–N(6)	71.44(17)
N(2)–Ag(1)–N(6)	130.74(17)	N(5)–Ag(1)–N(3)	129.21(18)
N(2)–Ag(1)–N(3)	71.81(13)	N(6)–Ag(1)–N(3)	125.03(18)
<i>Complex 3</i>			
Ag(1)–N(5)	2.257(3)	Ag(1)–N(2)	2.275(3)
Ag(1)–N(6)	2.401(3)	Ag(1)–N(1)	2.422(3)
N(5)–Ag(1)–N(2)	153.28(11)	N(5)–Ag(1)–N(6)	71.88(11)
N(2)–Ag(1)–N(6)	111.39(10)	N(5)–Ag(1)–N(1)	135.49(11)
N(2)–Ag(1)–N(1)	70.86(11)	N(6)–Ag(1)–N(1)	102.49(10)
<i>Complex 4</i>			
Ag(1)–N(4)	2.191(2)	Ag(1)–N(2)	2.305(2)
Ag(1)–N(3)	2.342(2)		
N(4)–Ag(1)–N(2)	131.75(9)	N(4)–Ag(1)–N(3)	156.06(9)
N(2)–Ag(1)–N(3)	72.13(8)		
<i>Complex 5</i>			
Ag(1)–N(4) <sup>#1</sup>	2.183(3)	Ag(1)–N(1)	2.257(3)
Ag(1)–N(2)	2.395(3)		
N(4) <sup>#1</sup> –Ag(1)–N(1)	159.98(11)	N(4) <sup>#1</sup> –Ag(1)–N(2)	127.81(10)
N(1)–Ag(1)–N(2)	72.19(9)		

Symmetry code for **5**: #1  $-x + 3/2, y - 1/2, -z + 1/2$ .

pyridyl rings of ligands, the strong absorption band at  $\sim 1575\text{ cm}^{-1}$  resulting from the skeletal vibrations of the aromatic rings of the free ligands blue-shifted to  $\sim 1600\text{ cm}^{-1}$  in the complexes. The results of elemental analysis are in agreement with the theoretical requirements of these complexes.

### 3.2. Crystal structures

$[\text{Ag}(\text{L}^1)_2](\text{ClO}_4)$  **1**. The crystal structure of **1** consists of discrete  $[\text{Ag}(\text{L}^1)_2]^+$  and  $\text{ClO}_4^-$ . The perspective view of **1** is shown in Fig. 1a and the selected bond distances and angles are listed in Table 2. The coordination geometry

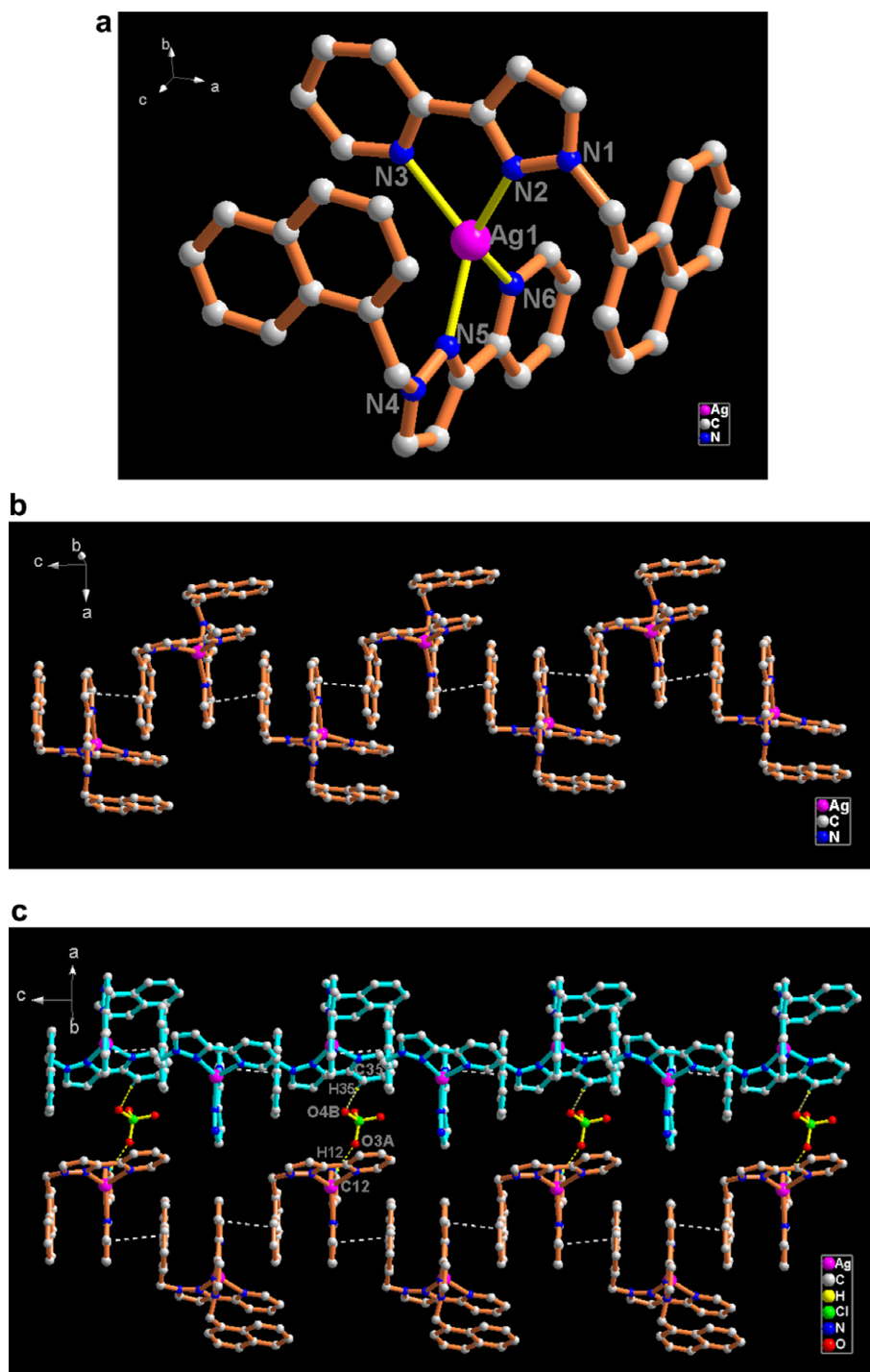


Fig. 2. View of (a) the coordination environment of Ag(I) in **2**, (b) the 1D chain arrayed by the intermolecular  $\pi \cdots \pi$  interactions and (c) the 2D network formed through inter-chain C–H  $\cdots$  O H-bonding interactions (partial naphthalene rings, H atoms, and  $\text{ClO}_4^-$  anions omitted for clarity).

around the Ag(I) center could be described as a distorted tetrahedron with the bond angles ranging from 71.20(2)° to 146.05(2)°. All the Ag–N bond distances [2.253(4)–2.416(4) Å] fall into the normal ranges for such coordination complexes (see Table 2) [26]. **L**<sup>1</sup> adopts *N,N*-bidentate chelating coordination mode to form two five-membered chelating cycles (Ag–N–C–C–N) with Ag(I) center, namely, Ag(1)–N(2)–C(10)–C(11)–N(3) and Ag(1)–N(5)–C(25)–C(26)–N(6) with the N–Ag–N angles of 72.31(2)° for N(2)–Ag(1)–N(3)° and 71.20(2)° for N(5)–Ag(1)–N(6), respectively.

It should be noted that, due to the flexibility of the methylene group, the phenyl group of **L**<sup>1</sup> can turn freely to offer a suitable space for intermolecular edge-to-face C–H... $\pi$  interaction with the pyridyl–pyrazole ring of another **L**<sup>1</sup> ligand from the adjacent [Ag(**L**<sup>1</sup>)<sub>2</sub>]<sup>+</sup> units [ $d = 2.7989$  and  $2.8489$  Å;  $A = 166.99^\circ$  and  $169.04^\circ$ ;  $d$  and  $A$  stand for the H... $\pi$  separations and C–H... $\pi$  angles in the C–H... $\pi$  patterns, respectively]. Additionally, the adjacent discrete [Ag(**L**<sup>1</sup>)<sub>2</sub>]<sup>+</sup> units are arranged into a one-dimensional (1D) chain by the combination of the weak intermolecular C–H... $\pi$  interaction mentioned above and  $\pi$ ... $\pi$  interactions between the pyridyl–pyrazole ring of one **L**<sup>1</sup> and pyridine ring of another distinct **L**<sup>1</sup> with the closest centroid–centroid distances of 3.580 Å, and the average interplanar separation of 3.440 Å and the dihedral angle of 1.5°, respectively (Fig. 1b) [27,28].

[Ag(**L**<sup>2</sup>)<sub>2</sub>](ClO<sub>4</sub>) **2**. The crystal structure of **2** consists of [Ag(**L**<sup>2</sup>)<sub>2</sub>]<sup>+</sup> and uncoordinated ClO<sub>4</sub><sup>−</sup>, which has a similar coordination geometry to that of **1**. The perspective view of the mononuclear entity in **2** with atomic labeling is given in Fig. 2a and the selected bond distances and angles are also listed in Table 2. Each Ag(I) center is four-coordinated by four N donors of pyridyl–pyrazole rings from two **L**<sup>2</sup> ligands, then giving a distorted tetrahedral geometry. All the Ag–N bond distances [2.293(5)–2.371(3) Å] are within the normal range expected for such coordination bond distances and angles around each Ag(I) center ranging from 71.44(2)° to 138.46(2)° (see Table 2) [26]. Moreover, the Ag–N distances formed by N(3) and N(6) of the pyridine rings [Ag–N(3) = 2.371(3) Å and Ag–N(6) = 2.370(5) Å] are a little longer than those formed by N(2) and N(5) of the pyrazole rings [Ag–N(2) = 2.302(3) Å and Ag–N(5) = 2.293(5) Å]. Similar to **1**, in **2**, **L**<sup>2</sup> also adopts *N,N*-bidentate chelating coordination mode to form two five-membered Ag–N–C–C–N cycles [Ag(1)–N(2)–C(14)–C(15)–N(3) and Ag(1)–N(5)–C(33)–C(34)–N(6) with the N–Ag–N angles of N(2)–Ag(1)–N(3) = 71.81(1)° and N(5)–Ag(1)–N(6) = 71.44(2)°, respectively].

However, different from **1**, in **2**, all the aromatic rings are almost parallel to each other to form a suitable space for intermolecular  $\pi$ ... $\pi$  interactions between the pyridyl–pyrazole and naphthalene rings from other **L**<sup>2</sup> ligands (Fig. 2b). Thus, the adjacent [Ag(**L**<sup>2</sup>)<sub>2</sub>]<sup>+</sup> units are arranged into 1D chain through the  $\pi$ ... $\pi$  interactions. The closest centroid–centroid distance, average interplanar

separation and dihedral angle are 3.520, 3.486 Å, and 2.2°, respectively (Fig. 2b) [27]. Furthermore, the adjacent 1D chains were linked together to form a quasi-2D network through the inter-chain C–H...O bonding between the O atoms of the free ClO<sub>4</sub><sup>−</sup> and H atoms of pyridine or pyrazole rings of distinct **L**<sup>2</sup> ligands (C(12)–H(12)...O(3A)) and (C(35)–H(35)...O(4B)) (Fig. 2c). The separations of C(12)...O(3A) and C(35)...O(4B) are 3.253 and 3.410 Å, with the angles for C(12)–H(12)...O(3A) and C(35)–H(35)...O(4B) of 151.98° and 173.81°, respectively (symmetry code A =  $-x + 1, -y + 1, -0.5 + z$ ; B =  $-x + 0.5, y - 0.5, z - 0.5$ , see Table 3) [29].

[Ag(**L**<sup>3</sup>)(HL<sup>3</sup>)](ClO<sub>4</sub>)<sub>2</sub>(CH<sub>3</sub>CN) **3**. Complex **3** consists of a discrete [Ag(**L**<sup>3</sup>)(HL<sup>3</sup>)<sub>2</sub>]<sup>2+</sup>, two ClO<sub>4</sub><sup>−</sup> and one CH<sub>3</sub>CN molecule (Fig. 3a). Similar to **1** and **2**, in **3**, the coordination geometry of Ag(I) is also a distorted tetrahedron coordinated by four N donors of two distinct **L**<sup>3</sup> ligands. All the Ag–N bond distances [2.257(3)–2.422(3) Å] are in the normal range for such analogous complexes [26] and the bond angles around each Ag(I) range from 70.86(1)° to 153.28(1)° (see Table 2). **L**<sup>3</sup> also adopts *N,N*-bidentate chelating coordination mode with Ag(I) center forming five-membered chelating cycles in which the N–Ag–N angles are 70.85(1)° for N(2)–Ag(1)–N(1)° and 71.89(1)° for N(5)–Ag(1)–N(6). However, **L**<sup>3</sup> does not use the N donor of its quinoline ring to coordinate to the Ag(I) center in the course of the formation of **3**, even though its electron density of N donor was much higher than those of 3-(2-pyridyl)pyrazole of **L**<sup>3</sup> (see below, Scheme 1), which may be due to the steric hindrance of the quinoline ring. It should be pointed out that in each mononuclear unit [Ag(**L**<sup>3</sup>)(HL<sup>3</sup>)<sub>2</sub>]<sup>2+</sup> of **3**, N(8) donor of quinoline ring in **L**<sup>3</sup> is protonated for the charge balance of the whole complex (Fig. 3a) and presents a strong hydrogen-bonding interac-

Table 3  
Hydrogen-bonding geometry (Å, °) for complexes 2–5

D–H...A	D–H	H...A	D...A	D–H...A
<b>2</b>				
C(12)–H(12)...O(3A)	0.930	2.403	3.253	151.98
C(35)–H(35)...O(4B)	0.930	2.484	3.410	173.81
<b>3</b>				
C(7)–H(7A)...O(1A)	0.930	2.517	3.349	148.92
C(34)–H(34A)...O(3A)	0.930	2.535	3.200	128.73
C(2)–H(2B)...O(2B)	0.930	2.585	3.462	157.27
C(8)–H(8C)...O(4C)	0.930	2.542	3.414	156.19
N(8)–H(8A)...O(5D)	0.860	1.975	2.766	152.42
<b>4</b>				
C(2)–H(2A)...O(4A)	0.930	2.540	3.450	166.08
C(11)–H(11A)...O(2B)	0.930	2.498	3.173	129.61
C(12)–H(12A)...O(2C)	0.930	2.600	3.395	143.80
C(13)–H(13A)...O(3C)	0.930	2.590	3.321	135.89
<b>5</b>				
C(8)–H(8A)...O(2A)	0.930	2.515	3.381	154.78

Symmetry code for **2**: A =  $-x + 1, -y + 1, z - 0.5$ , B =  $-x + 0.5, y - 0.5, z - 0.5$ ; for **3**: A =  $-x + 1, y - 0.5, -z + 0.5$ , B =  $-x + 1, -y, -z$ , C =  $-x + 1, -y, -z + 1$ , D =  $x, y - 1, z$ ; for **4**: A =  $-x, -y + 1, -z$ , B =  $1 - x, -y + 1, 1 - z$ , C =  $-x, -y + 1, 1 - z$ ; for **5**: A =  $x + 0.5, -y + 0.5, z + 0.5$ .

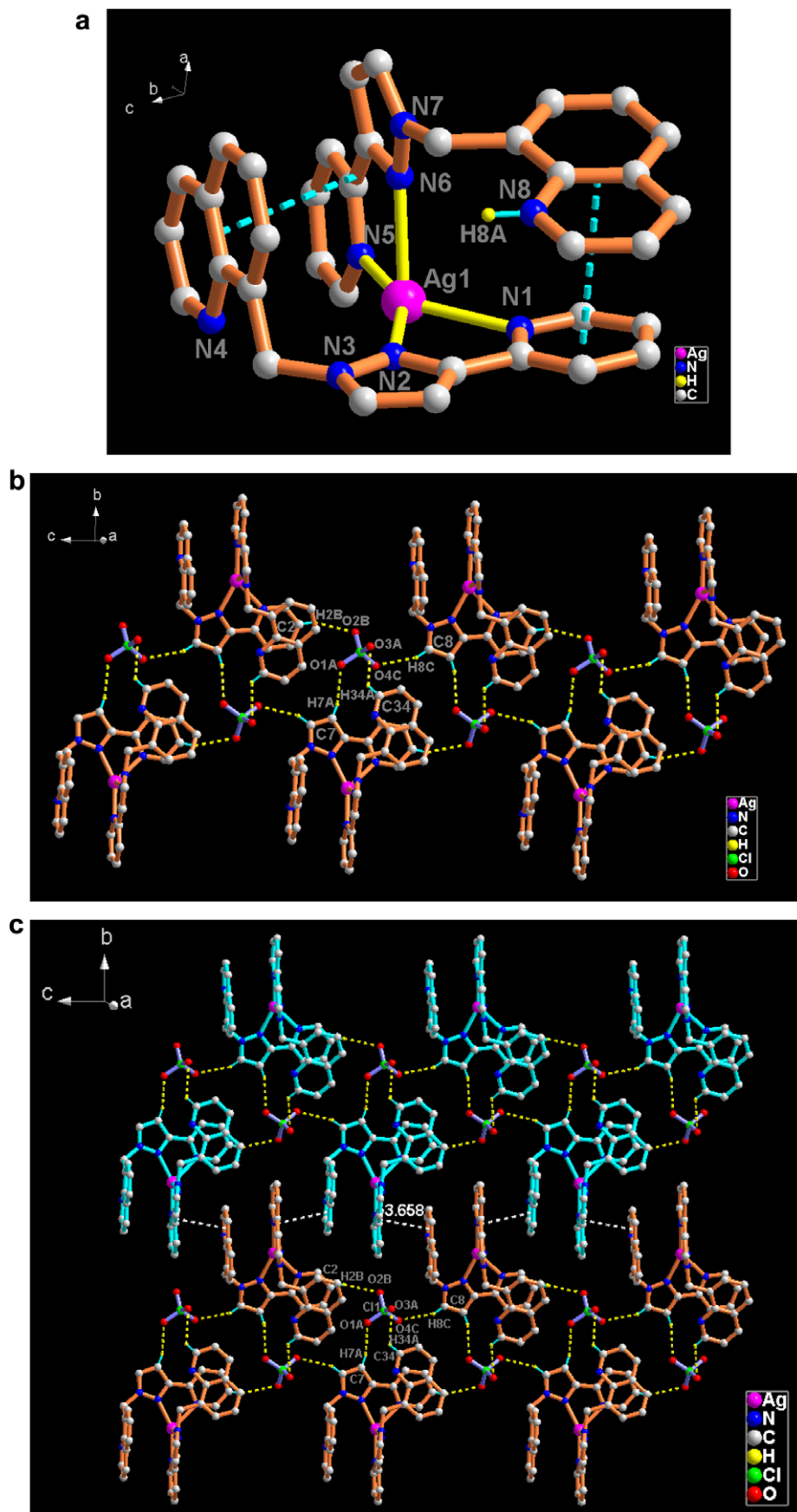
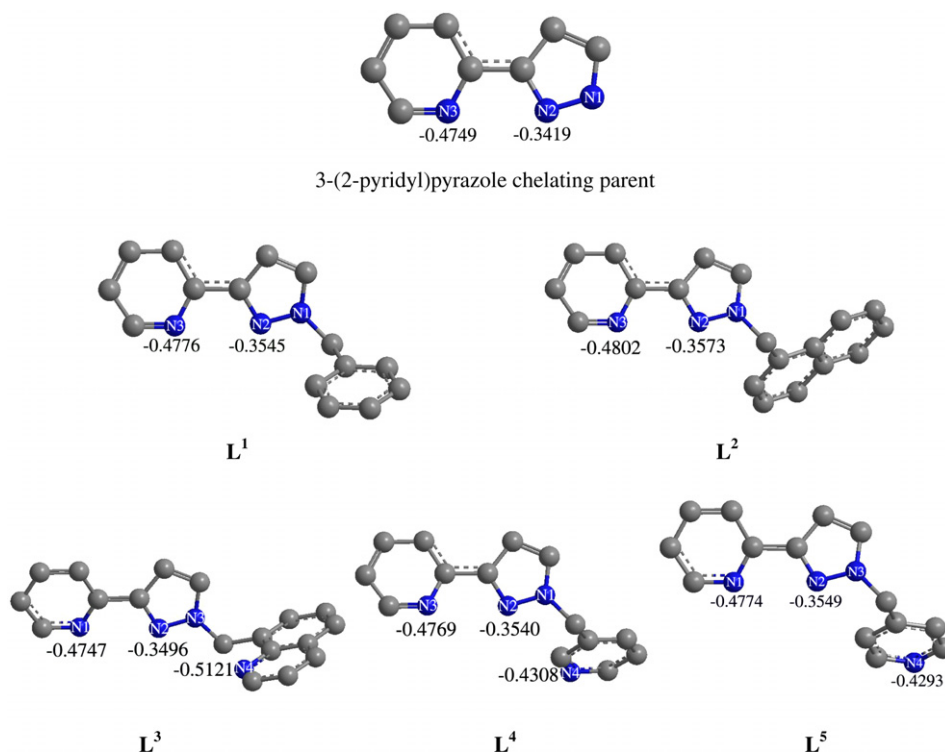


Fig. 3. View of (a) the coordination environment of Ag(I) in **3** with the intramolecular  $\pi \cdots \pi$  interactions, (b) the 1D chain constructed via  $\text{C-H} \cdots \text{O}$  H-bonding with  $\mu_4\text{-ClO}_4^-$  bridging mode and (c) the 2D network formed through inter-chain  $\pi \cdots \pi$  interactions (partial H atoms and  $\text{ClO}_4^-$  omitted for clarity).



Scheme 1. The optimized conformations for 3-(2-pyridyl)pyrazole and  $L^1$ – $L^5$  showing the calculated electron density distributions for N donors (H atoms omitted for clarity).

tions with the O(5D) atom of the uncoordinated  $\text{ClO}_4^-$  [the N(8)  $\cdots$  O(5D) and H(8A)  $\cdots$  O(5D) separations are 1.975 and 2.766 Å, N(8)–H(8A)  $\cdots$  O(5D) angle is 152.42°, symmetry code  $D = x, y - 1, z$  see Table 3]. Moreover, in **3**, the centroid–centroid separations, interplanar separations and dihedral angles between the pyridyl–pyrazole and quinoline rings from adjacent  $L^3$  ligands are falling into 3.595–3.618, 3.448–3.583 Å, and 2.4–13.3°, respectively, showing the obvious existence of the intramolecular  $\pi \cdots \pi$  interactions (see also Fig. 3a) [27].

Different from **1** and **2**, an interesting feature of **3** resides in the unique  $\mu_4$ - $\text{ClO}_4^-$  bridging mode, to link the  $[\text{Ag}(\text{L}^3)(\text{HL}^3)]^{2+}$  cationic units to form an extended 1D chain through C–H  $\cdots$  O bonding interactions between the O atoms of  $\text{ClO}_4^-$  and H atoms of the pyridine, pyrazole, and quinoline rings of distinct  $L^3$  ligands (Fig. 3b). The separations of C(7)  $\cdots$  O(1A), C(34)  $\cdots$  O(3A), C(2)  $\cdots$  O(2B), and C(8)  $\cdots$  O(4C) are 3.349, 3.200, 3.462, and 3.414 Å with the angles for C(7)–H(7A)  $\cdots$  O(1A), C(34)–H(34A)  $\cdots$  O(3A), C(2)–H(2B)  $\cdots$  O(2B), and C(8)–H(8C)  $\cdots$  O(4C) of 148.92°, 128.73°, 157.27°, and 156.19°, falling into the normal range of the C–H  $\cdots$  O bonding respectively (symmetry code  $A = -x + 1, y - 0.5, 0.5 - z; B = 1 - x, -y, -z; C = 1 - x, -y, 1 - z$  also see Table 3) [29].

In addition, the quinoline rings of  $L^3$  form the intermolecular  $\pi \cdots \pi$  interactions with the pyridyl–pyrazole rings from adjacent molecules, which further assemble the adjacent 1D chains into quasi-2D network, with the centroid–centroid separation, average interplanar separation and

dihedral angle being 3.658, 3.565 Å, and 3.1°, respectively (Fig. 3c) [27].

Complexes **1**–**3** have similar subunit and metal coordination geometries, however, their stacking patterns in the crystals are obviously different: **1** forms a linear 1D chain through intermolecular C–H  $\cdots$   $\pi$  and  $\pi \cdots \pi$  stacking interactions, while **2** and **3** are 2D network via intermolecular C–H  $\cdots$  O H-bonding and  $\pi \cdots \pi$  interactions. These results indicate that the different pendant aromatic groups in  $L^1$ – $L^3$  ligands may greatly influence the stacking mode of their complexes in the solid state.

$[\text{Ag}(\text{L}^4)](\text{ClO}_4)_2$  **4**. The structure of **4** consists of a centrosymmetric dinuclear  $[\text{Ag}_2(\text{L}^4)_2]^{2+}$  unit and two  $\text{ClO}_4^-$ . The dinuclear  $[\text{Ag}_2(\text{L}^4)_2]^{2+}$  cation (Fig. 4a) comprises two ligand  $L^4$  and two Ag(I) ions. Each Ag(I) center takes a slightly distorted trigonal planar geometry formed by three N donors, two from the pyridyl–pyrazole ring of one  $L^4$ , and one from the pendant pyridine ring of another  $L^4$ . All the Ag–N bond distances and bond angles around each Ag(I) center are in the normal range of such complexes [2.191(2)–2.342(2) Å and 72.13(8)–156.06(9)° region, respectively] (Table 2) [26]. Meanwhile, each uncoordinated  $\text{ClO}_4^-$  anion shows Ag  $\cdots$  O weak coordination with the Ag(I) centers (the Ag  $\cdots$  O distances being 2.933 and 3.183 Å).

In addition, the adjacent discrete dinuclear  $[\text{Ag}_2(\text{L}^4)_2]^{2+}$  units are assembled into a 1D chain by the combination of the weak face-to-face  $\pi \cdots \pi$  stackings (closest centroid–centroid separation of 3.758 Å between the pyridyl–pyrazole rings) and the C–H  $\cdots$  O H-bonding interactions

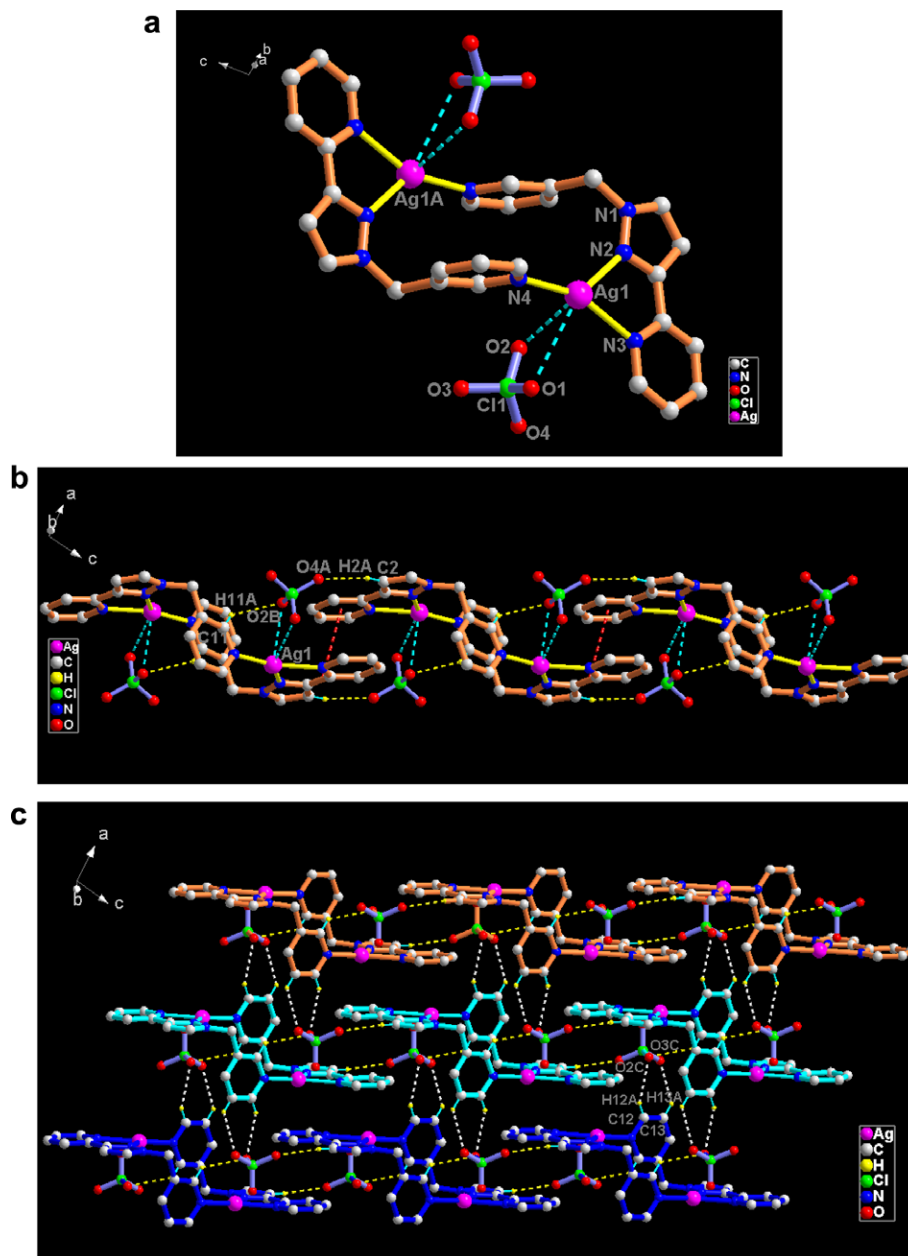


Fig. 4. View of (a) the coordination environment of Ag(I) in **4** with the intramolecular Ag $\cdots$ O weak interactions, (b) the 1D chain formed by the intermolecular C–H $\cdots$ O H-bonding and  $\pi \cdot \cdot \pi$  interactions between dinuclear subunits and (c) the 2D network formed through inter-chain C–H $\cdots$ O H-bonding interactions (partial H atoms and ClO $_4^-$  omitted for clarity).

between O atoms of the ClO $_4^-$  anions and H atoms of the pyridyl–pyrazole as well as pendant pyridine rings of distinct **L**<sup>4</sup> ligands [C(2)–H(2A)  $\cdots$  O(4A) and (C(11)–H(11A)  $\cdots$  O(2B))] (Fig. 4b). The separations of C(2)  $\cdots$  O(4A) and C(11)  $\cdots$  O(2B) are 3.450 and 3.173 Å, with the angles for C(2)–H(2A)  $\cdots$  O(4A) and C(11)–H(11A)  $\cdots$  O(2B) of 166.08° and 129.61°, respectively (symmetry code  $A = -x, -y + 1, -z$  and  $B = -x + 0.5, y - 0.5, z - 0.5$  see also Table 3) [29]. Also, the adjacent 1D chains were further linked to form a quasi-2D network through the intermolecular C–H $\cdots$ O bonding interactions between O atoms of the ClO $_4^-$  anions and H atoms of the pendant pyridine rings [C(12)–

H(12A)  $\cdots$  O(2C) and C(13)–H(13A)  $\cdots$  O(3C)] with the separations of 3.395 and 3.321 Å for C(12)  $\cdots$  O(2C) and C(13)  $\cdots$  O(3C) and the angles of 143.80° and 135.89° for C(12)–H(12A)  $\cdots$  O(2C) and C(13)–H(13A)  $\cdots$  O(3C), respectively (symmetry code  $C = -x, -y + 1, 1 - z$  see also Table 3) (Fig. 4c) [29].

$\{[\text{Ag}(\text{L}^5)](\text{ClO}_4)\}_\infty$  **5**. Different from **4**, the crystal structure of **5** consists of ClO $_4^-$  and 1D chain cations  $\{[\text{AgL}^5]^+\}_\infty$  (Fig. 5a and b). In the cationic chain, there is only one crystallographic independent Ag(I) center which, similar to **4**, adopts a distorted trigonal planar coordination geometry finished by three N donors, two from the pyridyl–pyrazole ring of one **L**<sup>5</sup> and one from

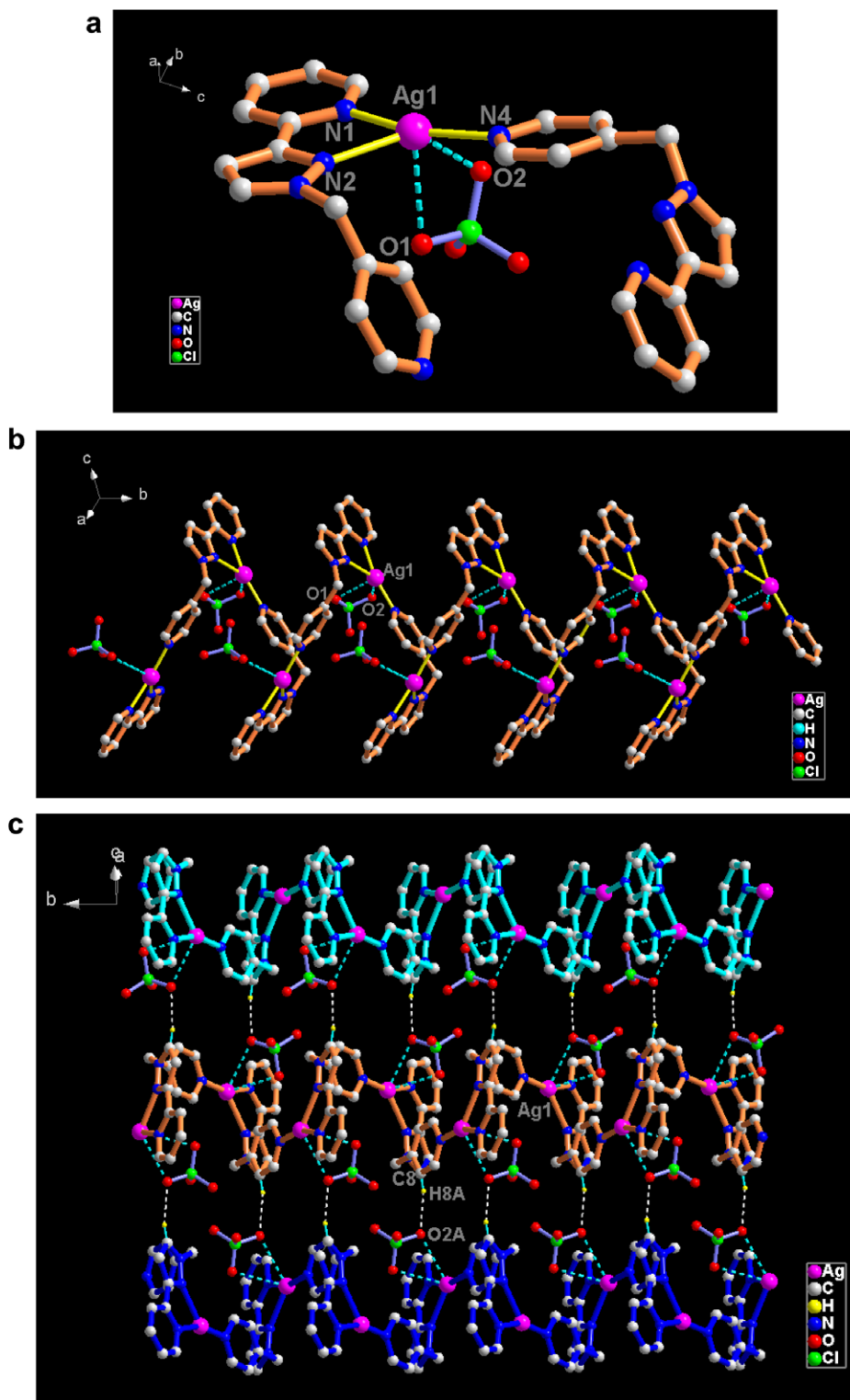


Fig. 5. View of (a) the coordination environment of Ag(I) in **5**, (b) the 1D chain structure with the intra-chain Ag...O weak interactions and (c) the 2D network formed through inter-chain C-H...O hydrogen-bonding interactions (partial H atoms and ClO<sub>4</sub><sup>-</sup> omitted for clarity).

the pendant pyridine ring of another L<sup>5</sup>. The free ClO<sub>4</sub><sup>-</sup> anions show weak coordination with Ag(I) centers with the Ag...O distances of 2.944 and 3.024 Å, respectively. The Ag–N bond distances [2.183(3)–2.395(3) Å] fall in the expected range for such complexes [26] and the

N–Ag–N angles in 72.19(9)–159.98(1)°. L<sup>5</sup> coordinates to the Ag(I) centers adopting *N,N*-bidentate chelating and terminal bridging modes, then resulting in an infinite helical chain with the intramolecular Ag...Ag separation of 7.787 Å.

Furthermore, the adjacent 1D chains are linked together to form a quasi-2D network through the co-effects of the weak Ag $\cdots$ O interaction aforementioned and the C–H $\cdots$ O H-bonding interactions between O atoms of the free ClO $_4^-$  anions and H atoms of the pendant pyridine rings [C(8)–H(8A) $\cdots$ O(2A)] with the separation of 3.381 Å for C(8) $\cdots$ O(8A) and the angle of 154.78° for C(8)–H(8A) $\cdots$ O(2A), respectively (symmetry code  $A = x + 0.5, -y + 0.5, z + 0.5$  see also Table 3) (Fig. 5c) [29].

In comparing with **4**, **5** does not form discrete structure but a 1D helical chain, which may be ascribed to the different positions of N donors in the pendant pyridine rings of **L**<sup>4</sup> and **L**<sup>5</sup> because the electron density of the three N donors are almost the same with each other based upon those theoretical results (see Scheme 1 and discussion below). In fact, the electron density and spatial positions of the coordinated N donor as well as the steric hindrance of the different aromatic pendant groups of ligands **L**<sup>1</sup>–**L**<sup>5</sup> may jointly affect the final crystal structures of **1**–**5**.

### 3.3. Theoretical computational results

In order to explore the underlying relationship between the electron density of these coordinated N donors in **L**<sup>1</sup>–**L**<sup>5</sup> ligands and the spatial structures of their complexes from the standpoint of electronic effect, ab initio and density functional theory (DFT) calculations of the five ligands **L**<sup>1</sup>–**L**<sup>5</sup>, as well as 3-(2-pyridyl)pyrazole for comparison, were performed. The full geometry optimizations for 3-(2-pyridyl)pyrazole and **L**<sup>1</sup>–**L**<sup>5</sup> based on the geometries of the coordinated ligands in **1**–**5** were carried out using DFT. The calculated electron density distributions for N donors of the free (3-(2-pyridyl)pyrazole) and **L**<sup>1</sup>–**L**<sup>5</sup> were shown in Scheme 1. The theoretical results show that the electron density distributions of the N donors in **L**<sup>1</sup>–**L**<sup>5</sup> are slightly increased after the different aromatic pendant groups are appended to 3-(2-pyridyl)pyrazole. The N donors of the pyridine ring carried negative charge ranging from 0.4747 to 0.4802, and those of N donors in pyrazole rings were from 0.3496 to 0.3573. Herein, it should be noted that the N donor of the quinoline ring in **L**<sup>3</sup> were not coordinated to Ag(I) in the formation of **3** although the electron density of its N donor was much higher than those of the free 3-(2-pyridyl)pyrazole and **L**<sup>1</sup>–**L**<sup>5</sup>, which may be ascribed to the steric hindrance of the quinoline ring in **L**<sup>3</sup>. On the other hand, in **L**<sup>4</sup> and **L**<sup>5</sup>, the electron density of these N donors are much the same with each other and the different crystal structures of them (diuclear structure for **L**<sup>4</sup> and 1D helical chain for **L**<sup>5</sup>) obviously result from the different positions of its N donors in the pyridine rings.

In conclusion, five new Ag(I) complexes based on five structurally related 3-(2-pyridyl)pyrazole-based ligands have been synthesized and characterized, which exhibits a systematic structural variation of coordination architectures. The results show that the structures of **1**–**5** could be affected by the coordination geometries of the pendant

aromatic groups. Meanwhile, various intra- or inter-molecular weak interactions, such as H-bonding, C–H $\cdots$  $\pi$  and  $\pi\cdots\pi$  interactions, also play important roles in the formation of **1**–**5**, especially in the aspect of linking the discrete subunits or low-dimensional entities into high-dimensional supramolecular networks. Moreover, the coordination behaviors of **L**<sup>1</sup>–**L**<sup>5</sup> ligands have been briefly investigated by DFT calculations and the results indicate that electron density or spatial position of coordinated N donors in the pendant aromatic groups of **L**<sup>1</sup>–**L**<sup>5</sup> ligands may jointly affect the final crystal structures, which offer us an effective means to construct unique supramolecular complexes with tailored structures.

### Acknowledgements

This work was supported by the National Natural Science Funds for Distinguished Young Scholars of China (No. 20225101) and NSFC (Nos. 20373028 and 20531040).

### References

- [1] (a) For examples S. Kitagawa, R. Kitaura, S. Noro, *Angew. Chem. Int. Ed.* 43 (2004) 2334;  
(b) M. Ruben, J. Rojo, F.J. Romero-Salguero, L.H. Uppadine, J.M. Lehn, *Angew. Chem. Int. Ed.* 43 (2004) 3644;  
(c) O.R. Evans, W.B. Lin, *Acc. Chem. Res.* 35 (2002) 511;  
(d) S.R. Seidel, P.J. Stang, *Acc. Chem. Res.* 35 (2002) 972;  
(e) B. Moulton, M.J. Zaworotko, *Chem. Rev.* 101 (2001) 1629;  
(f) P.J. Steel, *Acc. Chem. Res.* 38 (2005) 243.
- [2] (a) X. Zhao, B. Xiao, A.J. Fletcher, K.M. Thomas, D. Bradshaw, M.J. Rosseinsky, *Science* 306 (2004) 1012;  
(b) E.J. Schelter, A.V. Prosvirin, K.R. Dunbar, *J. Am. Chem. Soc.* 126 (2004) 15004.
- [3] (a) For examples M.L. Tong, Y.M. Wu, J. Ru, X.M. Chen, H.C. Chang, S. Kitagawa, *Inorg. Chem.* 41 (2002) 4846;  
(b) R. Sekiya, S. Nishikiori, *Chem. Eur. J.* 8 (2002) 4803;  
(c) X.H. Bu, M.L. Tong, H.C. Chang, S. Kitagawa, S.R. Batten, *Angew. Chem. Int. Ed.* 43 (2004) 192;  
(d) H. Hou, Y. Wei, Y. Song, L. Mi, M. Tang, L. Li, Y. Fan, *Angew. Chem. Int. Ed.* 44 (2005) 6067.
- [4] (a) J.S. Hall, J.G. Loeb, K.H. Shimizu, G.P.A. Yap, *Angew. Chem. Int. Ed.* 37 (1998) 121;  
(b) R.D. Schnebeck, E. Freisinger, B. Lippert, *Angew. Chem. Int. Ed.* 38 (1999) 168.
- [5] (a) M. Fujita *Comprehensive Supramolecular Chemistry*, vol. 9, Springer, Oxford, 1996;  
(b) W.Y. Sun, J. Fan, T. Okamura, J. Xie, K.B. Yu, N. Ueyama, *Chem. Eur. J.* 7 (2001) 2557.
- [6] (a) M.J. Zaworotko, *Angew. Chem. Int. Ed.* 39 (2000) 3052;  
(b) N.J. Melcer, G.D. Enright, J.A. Ripmeester, G.K.H. Shimizu, *Inorg. Chem.* 40 (2001) 4641.
- [7] N.W. Ockwig, O. Delgado-Friedrichs, M. O’Keeffe, O.M. Yaghi, *Acc. Chem. Res.* 38 (2005) 176.
- [8] P. Losier, M.J. Zaworotko, *Angew. Chem., Int. Ed., Engl.* 35 (1996) 2779.
- [9] E.S. Alekseyeva, A.S. Batsanov, L.A. Boyd, M.A. Fox, T.G. Hibbert, J.A.K. Howard, J.A.H. MacBride, A. Mackinnon, K. Wade, *J. Chem. Soc., Dalton Trans.* (2003) 475.
- [10] C.M.R. Juan, B. Lee, *Coord. Chem. Rev.* 183 (1999) 43.
- [11] T.N. Guru Row, *Coord. Chem. Rev.* 183 (1999) 81.
- [12] G.R. Desiraju, *Acc. Chem. Res.* 29 (1996) 441.

- [13] S.S. Kuduva, D.C. Craig, A. Nangia, G.R. Desiraju, *J. Am. Chem. Soc.* 121 (1999) 1936.
- [14] A.N. Khlobystov, A.J. Blake, N.R. Champness, D.A. Lemenovskii, A.G. Majouga, N.V. Zyk, M. Schröder, *Coord. Chem. Rev.* 222 (2001) 155.
- [15] I. Unamuno, J.M. Gutiérrez-Zorrilla, A. Luque, P. Román, L. Lezama, R. Calvo, T. Rojo, *Inorg. Chem.* 37 (1998) 6452.
- [16] M.C. Tse, K.K. Cheung, M.C.-W. Chan, C.M. Che, *Chem. Commun.* (1998) 2295.
- [17] Z.R. Bell, J.C. Jeffery, J.A. McCleverty, M.D. Ward, *Angew. Chem. Int. Ed.* 41 (2002) 2515.
- [18] (a) X.S. Shi, C.S. Liu, J.R. Li, Y. Guo, J.N. Zhou, X.H. Bu, *J. Mol. Struct.* 754 (2005) 71;  
(b) H. Zhang, C.S. Liu, X.H. Bu, M. Yang, *J. Inorg. Biochem.* 99 (2005) 1119;  
(c) R. Chen, C.S. Liu, H. Zhang, Y. Guo, M. Yang, X.H. Bu, *J. Inorg. Biochem.* (2006), doi:10.1016/j.jinorgbio.2006.11.001.;  
(d) R.Q. Zou, C.S. Liu, Z. Huang, T.L. Hu, X.H. Bu, *Cryst. Growth Des.* 6 (2006) 99.
- [19] (a) H. Brunner, T. Scheck, *Chem. Ber.* 125 (1992) 701;  
(b) Y. Lin, S.A. Lang, *J. Heterocycl. Chem.* 14 (1977) 345;  
(c) C.S. Liu, X.S. Shi, J.R. Li, J.J. Wang, X.H. Bu, *Cryst. Growth Des.* 6 (2006) 656;  
(d) X.H. Bu, D.L. An, Y.T. Chen, M. Shionoya, E. Kimura, *J. Chem. Soc. Dalton Trans.* (1995) 2289.
- [20] (a) Z.R. Bell, L.P. Harding, M.D. Ward, *Chem. Comm.* (2003) 2432;  
(b) D.A. McMorran, P.J. Steel, *Chem. Comm.* (2002) 2120;  
(c) M.J. Hinner, M. Grosche, E. Herdtweck, W.R. Thiel, *Z. Anorg. Allg. Chem.* 629 (2003) 2251.
- [21] Bruker AXS, SAINT Software Reference Manual, Madison, WI, 1998.
- [22] G.M. Sheldrick, SADABS, Siemens Area Detector Absorption Corrected Software, University of Göttingen, Germany, 1996.
- [23] G.M. Sheldrick, SHELXTL NT, Version 5.1; Program for Solution and Refinement of Crystal Structures, University of Göttingen, Germany, 1997.
- [24] Gaussian 03, Revision C.01, M.J. Frisch, G.W. Trucks, H.B. Schlegel, G.E. Scuseria, M.A. Robb, J.R. Cheeseman, J.A. Montgomery, J.T. Vreven, K.N. Kudin, J.C. Burant, J.M. Millam, S.S. Iyengar, J. Tomasi, V. Barone, B. Mennucci, M. Cossi, G. Scalmani, N. Rega, G.A. Petersson, H. Nakatsuji, M. Hada, M. Ehara, K. Toyota, R. Fukuda, J. Hasegawa, M. Ishida, T. Nakajima, Y. Honda, O. Kitao, H. Nakai, M. Klene, X. Li, J.E. Knox, H.P. Hratchian, J.B. Cross, C. Adamo, J. Jaramillo, R. Gomperts, R.E. Stratmann, O. Yazyev, A.J. Austin, R. Cammi, C. Pomelli, J.W. Ochterski, P.Y. Ayala, K. Morokuma, G.A. Voth, P. Salvador, J.J. Dannenberg, V.G. Zakrzewski, S. Dapprich, A.D. Daniels, M.C. Strain, O. Farkas, D.K. Malick, A.D. Rabuck, K. Raghavachari, J.B. Foresman, J.V. Ortiz, Q. Cui, A.G. Baboul, S. Clifford, J. Cioslowski, B.B. Stefanov, G. Liu, A. Liashenko, P. Piskorz, I. Komaromi, R.L. Martin, D.J. Fox, T. Keith, M.A. Al-Laham, C.Y. Peng, A. Nanayakkara, M. Challacombe, P.M.W. Gill, B. Johnson.
- [25] (a) A.D. Becke, *J. Chem. Phys.* 98 (1993) 5648;  
(b) C. Lee, W. Yang, R.G. Parr, *Phys. Rev. B* 37 (1988) 785.
- [26] (a) A.G. Orpen, L. Brammer, F.H. Alen, O. Kennard, D.G. Watson, R. Taylor, *J. Chem. Soc., Dalton Trans.* (1989) S1–S83;  
(b) M. O’Keeffe, N.E. Brese, *J. Am. Chem. Soc.* 113 (1991) 3226.
- [27] (a) C. Janiak, *J. Chem. Soc. Dalton Trans.* (2000) 3885;  
(b) S.M. Malathy Sony, M.N. Ponnuswamy, *Cryst. Growth Des.* 6 (2006) 736;  
(c) H. Liu, M. Du, *J. Mol. Struct.* 607 (2002) 143.
- [28] (a) P. Hobza, Z. Havlas, *Chem. Rev.* 100 (2000) 4253;  
(b) M.J. Calhorda, *Chem. Commun.* (2000) 801;  
(c) C.D. Abernethy, C.L.B. Macdonald, A.H. Cowley, J.A.C. Clyburne, *Chem. Commun.* (2001) 61.
- [29] G.R. Desiraju, T. Steiner, *The Weak Hydrogen Bond in Structural Chemistry and Biology*, Oxford University Press, Oxford, 1999.